Journal of Zhejiang University-SCIENCE A (Applied Physics & Engineering)
ISSN 1673-565X (Print); ISSN 1862-1775 (Online)
www.zju.edu.cn/jzus; www.springerlink.com
E-mail: jzus@zju.edu.cn

A simple approach for determining the preload of a wire race ball bearing*

Xiao-biao SHAN[†1], Li-li WANG[2], Tao XIE[†‡1], Wei-shan CHEN[1]

([1]*School of Mechatronics Engineering, Harbin Institute of Technology, Harbin 150001, China*)

([2]*College of Science, Northeast Forestry University, Harbin 150040, China*)

[†]E-mail: shanxiaobiao@hit.edu.cn; xietao@hit.edu.cn

Received Sept. 25, 2009; Revision accepted Mar. 4, 2010; Crosschecked June 10, 2010

Abstract: Wire race ball bearings have been widely used in high-tech weapons. The preload of a wire race ball bearing is crucial in engineering applications. In this study, a more effective approach is proposed for exact determination of the wire race ball bearing preload. A new mathematical model of the preload and the starting torque of the wire race ball bearing was built using the theorem of the 3D rolling friction resistance and the non-conforming contact theory. Employing a wire race ball bearing with a 1000 mm diameter used in a specific type of aircraft simulating rotary table, the numerical analysis in MATLAB® showed that the preload magnitude can be controlled in the range of 130–140 μm. As verification, the experimental results were in agreement with the theoretical results, and confirm the feasibility of this method. This new approach is more exact in the preload range of 10–158 μm than that computed by the numerical method reported in our previous work (Shan *et al*., 2007b). This implies that the present method contributes to more effectively preventing rolling noise, overturning moments and wear of the wire race ball bearing. The current research provides critical technical support for the engineering application of wire race ball bearings with large diameters.

Key words: Wire race ball bearing, Rolling friction, Starting torque, Contact interface
doi:10.1631/jzus.A0900583 **Document code:** A **CLC number:** TH133.33

1 Introduction

In the last 10 years the wire race ball bearing has been extensively used in the field of high-tech weaponry because of its low inertia, high rigidity, high precision, and average effect of errors and uniform temperatures (Shi, 2004; Fan, 2005). The preload of a wire race ball bearing plays a very important role in engineering applications (Shan *et al*., 2007a). The traditional method for adjusting the preload is to adjust the thickness of the shims by trial and error, the process of which relies heavily on personal experience and skill of the engineers. The traditional method inevitably leads to rolling noise, overturning moments, and wear.

To overcome the above problems, Shan *et al*. (2007b) developed a numerical method based on the frictionless non-conforming contact theory to construct the preload magnitude range of the wire race ball bearing. Even with this method, because the preload range is too wide, determining preload remains a challenge, and to an ongoing extent, engineers still have to adjust the thickness of the shims by trial and error. In fact, the friction torque in the Hertzian contacts depends upon the preload to a considerable extent (Poritsky *et al.*, 1947). It is well known that the rolling of a ball is a cyclical process, as the stress field resulting from the ball contact moves with the ball (Drutowski, 1959; Williams, 2005). The equilibrium rolling force increases rapidly once the contact stress becomes large enough to cause plastic deformation on initial rolling (Drutowski,

‡ Corresponding author

* Project supported by the National Natural Science Foundation of China (No. 50905039), and the Natural Science Foundation of Heilongjiang Province (No. E200924), China

1959; Willner, 2004). Accordingly, the above factors, including the normal contact load, the tangential friction, the contact stress field, and even the ball and race materials and the surface finish are directly associated with the friction torque of a wire race ball bearing. In fact, the friction torque of a wire race ball bearing is of significant importance and interest (Jones, 1952; Drutowski, 1959; 1962; Drutowski and Mikus, 1960). Therefore, the preload problem of a wire race ball bearing should be treated as a non-conforming rolling contact problem with friction.

The objective of this work is to explore a more effective approach for more precisely and accurately determining the preload of a wire race ball bearing. Based on the theories of both the rolling friction resistance and the non-conforming contact, the mathematical model incorporating starting torque and preload magnitude will be presented as follows. As an example, a wire race ball bearing is used in a specific type of aircraft simulating rotary table (Fig. 1) for the modeling and experimental verification.

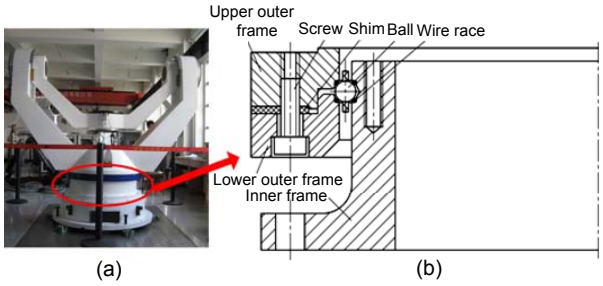

Fig. 1 Wire race ball bearing used in aircraft simulating rotary table
(a) Simulating rotary table; (b) Sketch of the wire race ball bearing

2 Mathematical modeling

2.1 Wire race ball bearing kinematics

It is well known that rolling friction is a complex problem and many factors may affect the value of rolling friction (Zhu and Yu, 2003). From the aspect of the energy loss, the primary friction losses in a wire race ball bearing consist of: (1) sliding friction losses in the contacts between the rolling elements and the raceways; (2) hysteresis losses due to the damping capacity of the raceway and the ball material; (3) sliding friction losses between the separator and its locating race surface and between the separator pockets and the rolling elements (Anderson, 1964). It is impossible, however, to take all factors into account during mathematical modeling. Hence, several assumptions are needed during the modeling procedure: (1) the case of dry friction is considered. Therefore, the viscous friction due to the lubrication was ignored; (2) the contact friction between the cage and the balls is ignored for its uncertainty and complexity; (3) the relative movement between balls and wires is regarded as the pure rolling at the start of revolution. Namely, the sliding friction between the contact bodies is assumed to be negligible; and, (4) it is assumed that the coefficient of rolling frictional resistance does not change with the normal contact pressure between balls and wires.

Accordingly, by treating the contact model as a quasi-static model associated with the rolling resistance (Lamon *et al*., 2004), the contact bodies (the ball and the wire) are mainly subjected to a normal contact load P, and a relative motion trend caused by a horizontal force F_v. In this case, contact deformation between the ball and the wire occurs. The contact point is expanded into a contact zone A (Fig. 2a).

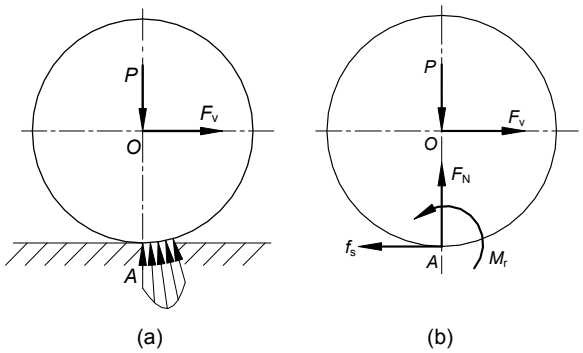

Fig. 2 Sketch of the rolling frictional resistance
(a) Rolling contact zone; (b) Moment of rolling frictional resistance couple

Thus, the rolling frictional resistance moment of couple M_r, the frictional force f_s, and the normal reaction force F_N in relationship to each other can be obtained (Fig. 2b). Therefore, according to the theorem of rolling frictional resistance, M_r is proportional to F_N. It can be expressed as

$$M_r=\xi F_N, \tag{1}$$

where ξ is the coefficient of rolling frictional resistance (m), which relates the normal contact force to

the rolling frictional resistance torque (Samper *et al*., 1999); M_r is the moment of rolling frictional resistance couple (N·m); and F_N is the normal contact force (N).

It is worth emphasizing that the exact value of ξ should be determined by the experiments. It will be described in Section 3.

Consequently, Fig. 3 illustrates the schematic drawing of the contact status. Fig. 4 shows the equivalent drawing of the space force couple for the contact between one ball and four wire races. From Fig. 4, the moment of rolling frictional resistance couple at the jth contact point on the ith ball, M_{rij}, can be described as

$$M_{rij}=\xi F_{ij}, \tag{2}$$

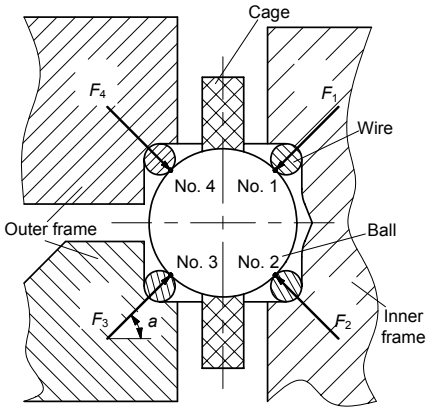

Fig. 3 Schematic drawing of the contact status
F_j ($1\leq j\leq 4$) is the contact force at the jth contact point (N), and α denotes the contact angle (rad)

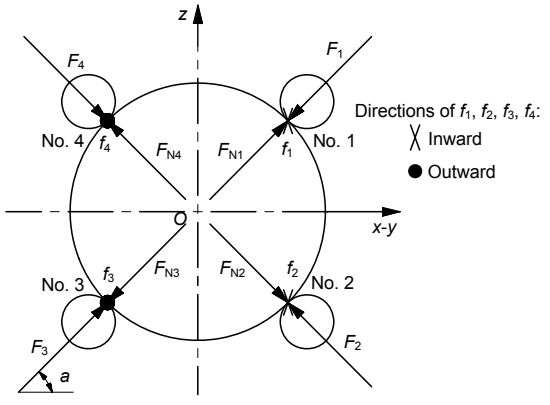

Fig. 4 Equivalent drawing of the space force couple for the contact between one ball and four wire races
F_j ($1\leq j\leq 4$) is the contact force at the jth contact point (N); F_{Nj} ($1\leq j\leq 4$) is the contact reaction force at the jth contact point (N); f_j ($1\leq j\leq 4$) is the frictional force at the jth contact point (N); and α is the contact angle (rad)

where i and j are integral numbers, $1\leq i\leq Z$ (Z denotes the number of balls), $1\leq j\leq 4$; and F_{ij} denotes the contact force at the jth contact point on the ith ball.

2.2 Bearing torque

The total equivalent frictional moment of couple for the bearing, M_{zr}, can be obtained:

$$M_{zr}=\sum_{i=1}^{Z}\sum_{j=1}^{4}M_{zrij}=\sum_{i=1}^{Z}\sum_{j=1}^{4}\xi F_{ij}\cos\alpha, \tag{3}$$

where α denotes the contact angle of the bearing (rad); M_{zrij} is the equivalent moment of rolling frictional resistance couple at the jth contact point on the ith ball (N·m).

Therefore, according to the relationship between the contact load and the contact deformation derived by Johnson (1985), the descriptions of the frictional starting torque for the wire race ball bearing, M_s, concerning the contact forces and the contact deformation at four contact points can be obtained as

$$M_s=M_{zr}=\xi Z(F_1+F_2+F_3+F_4)\cos\alpha, \tag{4}$$

where F_j ($1\leq j\leq 4$) denotes the contact force at the jth contact point (N), $F_1=K_i\delta_1^{3/2}$, $F_2=K_i\delta_2^{3/2}$, $F_3=K_o\delta_3^{3/2}$, $F_4=K_o\delta_4^{3/2}$, δ_j ($1\leq j\leq 4$) denotes the contact deformation at the jth contact point (m). The stiffness coefficients K_i and K_o are:

$$K_i=\sqrt{\frac{16E^{*2}R_{ei}}{9F_{2i}^3(e)}}, \tag{5}$$

$$K_o=\sqrt{\frac{16E^{*2}R_{eo}}{9F_{2o}^3(e)}}. \tag{6}$$

The specific definition of the parameters E^*, R_{ei}, R_{eo}, $F_{2i}(e)$ and $F_{2o}(e)$ are given in our previous work (Shan *et al*., 2007b).

Owing to considering the starting torque of the bearing, the external axial load, F_a, is zero. Accordingly, the following equilibrium equation can be obtained:

$$Z(F_1\sin\alpha-F_2\cos\alpha)+G_o=0, \tag{7}$$

where G_o is the gravity of the outer framework (N), and $F_1=F_3$, $F_2=F_4$.

Therefore, according to Eqs. (4) and (7), the contact forces are

$$F_1=\frac{1}{Z(\sin\alpha+\cos\alpha)}\left(\frac{M_s}{2\xi}-G_o\right), \tag{8}$$

$$F_2=\frac{1}{Z(\sin\alpha+\cos\alpha)}\left(\frac{M_s\tan\alpha}{2\xi}+G_o\right). \tag{9}$$

Finally, according to the definition of preload magnitude given in our previous work (Shan *et al*., 2007b), the relationship between the preload magnitude and the frictional starting torque can be expressed as

$$\begin{aligned}\delta&=\left[\left(\frac{F_1}{K_i}\right)^{2/3}+\left(\frac{F_2}{K_i}\right)^{2/3}+\left(\frac{F_3}{K_o}\right)^{2/3}+\left(\frac{F_4}{K_o}\right)^{2/3}\right]\cos\alpha\\&=\frac{\cos\alpha}{\left[Z(\sin\alpha+\cos\alpha)\right]^{2/3}}(K_i^{-2/3}+K_o^{-2/3})\\&\quad\times\left[\left(\frac{M_s}{2\xi}-G_o\right)^{2/3}+\left(\frac{M_s\tan\alpha}{2\xi}+G_o\right)^{2/3}\right].\end{aligned} \tag{10}$$

The validity of this mathematical model is verified by experiment as follows.

3 Experimental

A wire race ball bearing with a diameter of approximately 1000 mm diameter was used in a specific type of aircraft simulating rotary table. The bearing was fixed on the experimental platform (1600 mm ×2500 mm). Table 1 lists the geometry and material properties of the bearing. Fig. 5 shows the diagrammatic sketch of the measurement system for the starting torque. In this figure, the computer, in fact, refers to the process of the numerical programming and solving.

It is widely known that the most common finishing operation of shims is mechanical grinding with abrasives. Therefore, the 24 pieces of shims (fan-shaped, angle of the sector is 15°, as shown in Fig. 6) were simultaneously ground on a surface grinding machine. The preload magnitude of the bearing was controlled by grinding the two surfaces of the shims. The different thicknesses of the shims corresponded to the different preload magnitudes (Their relationship will be discussed in Section 4). The measures of the starting torque at different preloads were obtained.

Table 1 Geometry and material properties of the bearing

Parameter	Value
Pitch diameter of the bearing (mm)	889.6
Number of balls	90
Diameter of the wire race (mm)	3.0
Diameter of the ball (mm)	14.288
Contact angle of the bearing (rad)	π/4
Modulus of the wire race (GPa)	219.4
Modulus of the ball (GPa)	208
Poisson's ratio of the wire	0.3
Poisson's ratio of the ball	0.3
Material of the wire	T8MnA
Material of the ball	GGr15
Rockwell C hardness of the wire	51
Rockwell C hardness of the ball	67
Gravity of the outer framework (N)	806.27

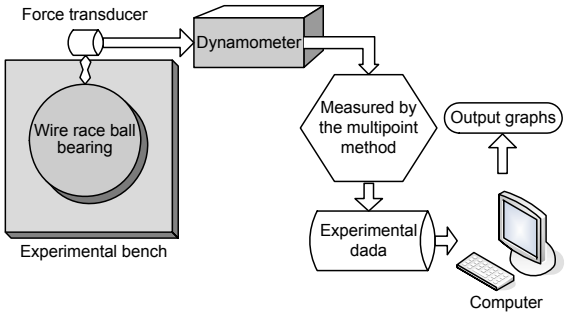

Fig. 5 Diagrammatic sketch of the measurement system for the starting torque

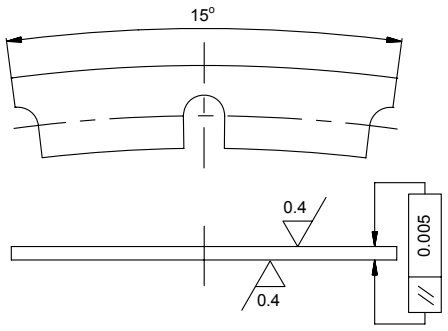

Fig. 6 Sketch map of a shim

Fig. 7 shows the experimental measuring system of the starting torque. The force transducer (CLF2-L2-500 kg, Liye Sensor Co. Ltd., China) was fixed on the outer frame of the wire race ball bearing. The signal of the force transducer was inputted into

the digital dynamometer (CL-2, Xinheng Electronic Technology Co. Ltd., China). The values of the force can be digitally displayed and directly recorded.

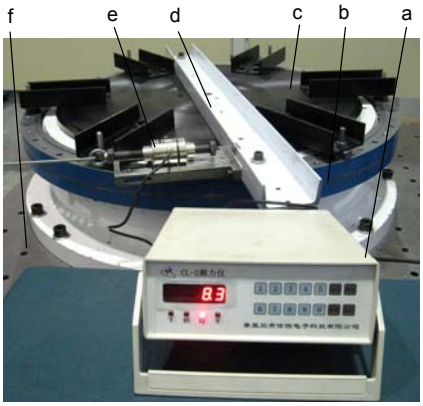

a: dynamometer; b: wire race ball bearing; c: rotating disc; d: steel channel beam; e: force transducer; f: experimental bench

Fig. 7 Experimental measuring system of the starting torque

In addition, a point worth emphasizing is that the multipoint measuring method and the arithmetical method was employed during the experiments to the minimize errors deriving from two aspects: (1) the error resulting from the machining; (2) the error caused by the inhomogeneous deformation of the wires.

4 Results and discussion

4.1 Experimental results

A numerical program was developed in MATLAB®, based on the above mathematical model, the parameters in Table 1 and the experimental data. Hence, the nonlinear relationship among the starting torque, the preload magnitude and the coefficient of rolling frictional resistance were obtained (Fig. 8).

From Fig. 8, one can see that the starting torque increases nonlinearly with the preload magnitude, and that the coefficient of rolling frictional resistance has a prominent nonlinear influence on the starting torque. In fact, this result is in good agreement with current engineering practice.

Table 2 shows the experimental data with respect to the preload, the starting torque and the contact loads between the contact bodies. It is worth mentioning that as long as the bolts are used to impose a preload during the experiments, it is probable that a misalignment or overturning moment of the bearing can occur when an inexperienced operator is assembling the wire race ball bearing. To overcome the experimental error in this regard, the bolts should be tightened evenly and symmetrically using a torque spanner.

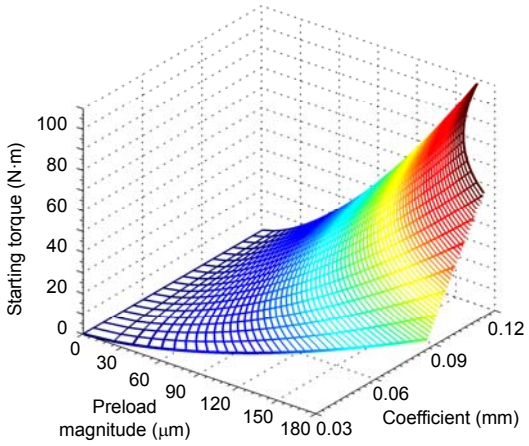

Fig. 8 Theoretical relationship among the starting torque, the preload magnitude and the coefficient of rolling frictional resistance

Thus, the experimental starting torque can be presented as follows:

$$M_{sn}=2\xi Z(F_{1n}+F_{2n})\cos\alpha+M_{\mathrm{u}}, \qquad (11)$$

where n is the group number of the experimental data, $1\leq n\leq 9$; M_{sn}, F_{1n} and F_{2n} denote the experimental starting torque and the contact loads listed in Table 2; M_{u} presents the frictional resistance torque caused by the unconsidered factors in the developed mathematical model. Incidentally, during the experiments, it was necessary to consider why the starting torque of a wire race ball bearing is higher than the running torque. In fact, according to the definition of the rolling frictional moment of the couple, it can be shown that the roller is in the critical state of equilibrium at the moment of starting. Simultaneously, the rolling frictional moment of a couple reaches its maximum. Therefore, the starting torque of the wire race ball bearing is higher than the running torque.

To minimize errors, the method of grouping and the arithmetical method were proposed during processing experimental data. Therefore, the coefficient of rolling frictional resistance can be defined as follows:

Table 2 Theoretical and experimental results with respect to the preload magnitude

h (mm)	Theoretical result												Experimental result	
	δ (μm)	F_1 (N)	F_2 (N)	δ_1 (μm)	δ_2 (μm)	δ_3 (μm)	δ_4 (μm)	P_{01} (GPa)	P_{02} (GPa)	P_{03} (GPa)	P_{04} (GPa)	M_{sc} (N·m)	M_{bm} (N·m)	M_{sm} (N·m)
3.99	10	45.93	58.60	3.25	3.82	3.25	3.82	2.504	2.716	2.504	2.715	1.37	17.33	0.01
3.98	20	141.17	153.84	6.87	7.27	6.87	7.27	3.640	3.746	3.640	3.746	3.85	21.19	3.86
3.96	40	410.76	423.43	14.00	14.29	14.00	14.28	5.197	5.250	5.197	5.250	10.90	29.62	12.30
3.94	60	759.91	772.56	21.10	21.33	21.10	21.33	6.380	6.415	6.379	6.415	20.02	37.30	19.97
3.92	80	1173.36	1186.03	28.18	28.39	28.18	28.38	7.374	7.401	7.373	7.400	30.83	42.43	25.11
3.90	100	1642.34	1655.01	35.27	35.45	35.26	35.44	8.249	8.270	8.248	8.269	40.81	51.73	34.41
3.88	120	2160.90	2173.57	42.35	42.51	42.34	42.51	9.039	9.057	9.038	9.056	50.63	75.31	57.99
3.86	140	2724.69	2737.36	49.42	49.58	49.42	49.57	9.765	9.780	9.764	9.779	71.36	99.40	82.08
3.84	160	3330.34	3343.01	56.50	56.64	56.49	56.64	10.441	10.454	10.440	10.453	87.19	106.85	89.53

h: shim thickness; δ_j ($1\leqslant j\leqslant 4$): contact deformation at the jth contact point; P_{0j} ($1\leqslant j\leqslant 4$): the maximum Hertz stress at the jth contact point; M_{sc}: calculated bearing torque; M_{bm}: measured bearing torque; M_{sm}: measured starting torque

$$\xi=\frac{\overline{M_s^{II}}-\overline{M_s^{I}}}{2Z\left[\left(\overline{F_1^{II}}+\overline{F_2^{II}}\right)-\left(\overline{F_1^{I}}+\overline{F_2^{I}}\right)\right]\cos\alpha}, \tag{12}$$

where $\overline{M_s^{I}}$ is the mean value of the first group of measured bearing torques, and $\overline{M_s^{I}}=\frac{1}{4}\sum_{n=1}^{4}M_{sn}$; $\overline{M_s^{II}}$ is the mean value of the second group of measured bearing torques, and $\overline{M_s^{II}}=\frac{1}{5}\sum_{n=5}^{9}M_{sn}$; $\overline{F_1^{I}}+\overline{F_2^{I}}$ is the sum of the mean values of the first group of contact loads F_1 and F_2, and $\overline{F_2^{I}}+\overline{F_2^{I}}=\frac{1}{4}\sum_{n=1}^{4}\left(F_{1n}+F_{2n}\right)$; $\overline{F_1^{II}}+\overline{F_2^{II}}$ is the sum of the mean values of the second group of contact loads F_1 and F_2, and $\overline{F_1^{II}}+\overline{F_2^{II}}=\frac{1}{5}\sum_{n=5}^{9}\left(F_{1n}+F_{2n}\right)$.

Furthermore, the frictional resistance torque caused by the unconsidered factors in the developed mathematical model can be obtained:

$$M_u=\overline{M_s}-2\xi Z\left(\overline{F_1}+\overline{F_2}\right)\cos\alpha, \tag{13}$$

where $\overline{M_s}$ is the mean value of the measured bearing torques, and $\overline{M_s}=\frac{1}{9}\sum_{n=1}^{9}M_{sn}$; $\overline{F_1}+\overline{F_2}$ is the sum of the mean values of the contact loads F_1 and F_2, and $\overline{F_1}+\overline{F_2}=\frac{1}{9}\sum_{n=1}^{9}(F_1+F_2)$.

Accordingly, the coefficients of rolling frictional resistance ξ and the frictional resistance torque caused by the unconsidered factors during modeling M_u can be obtained (Table 3).

Table 3 Results of the coefficients of rolling frictional resistance and the frictional resistance torque

Parameter	Value	Parameter	Value
$\overline{M_s^{I}}$ (N·m)	26.3600	$\overline{M_s^{II}}$ (N·m)	75.1440
$\overline{F_1^{I}}+\overline{F_2^{I}}$ (N)	691.5500	$\overline{F_1^{II}}+\overline{F_2^{II}}$ (N)	4425.3220
$\overline{M_s}$ (N·m)	53.4622	M_u (N·m)	17.3245
ξ ($\times10^{-4}$ m)	1.0265		

Fig. 9a illustrates the theoretical and experimental curves of the relationship between starting torque and preload magnitude. From Fig. 9a, it is determined that:

1. The starting torque increases with the increase of the preload magnitude.

2. The experimental curve is an S-shaped curve. It reveals that the complex contact deformation behaviors (elastic, elastic-plastic and plastic) occur in the interacting surfaces between the wires and the balls (Kogut and Etsion, 2002; Gao *et al*., 2006; Jamari and Schipper, 2006; 2007).

3. The friction loss in rolling was believed to be required to overcome the interfacial slip which

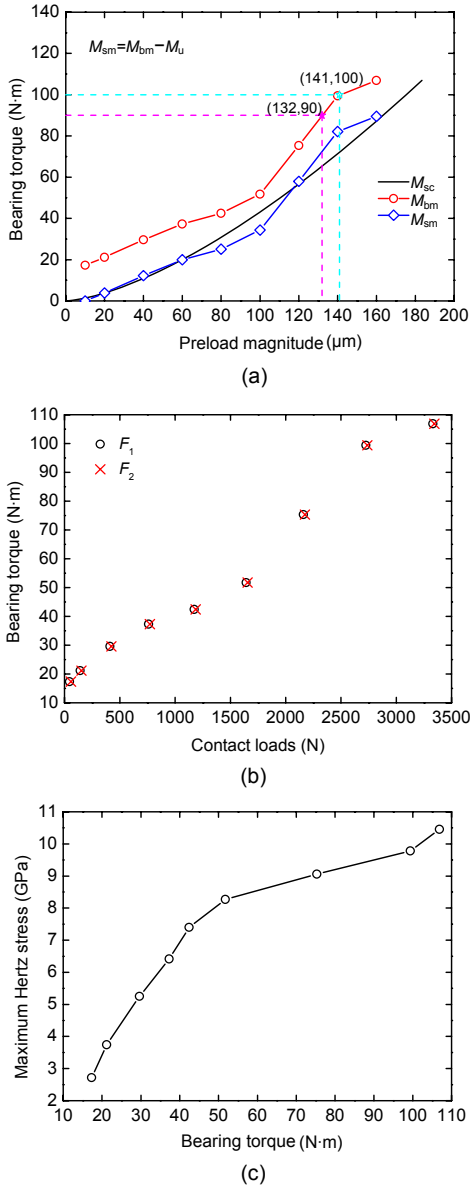

Fig. 9 Theoretical and experimental results regarding the relationship between bearing torques and the preload magnitude, contact loads, and the maximum Hertz stresses
(a) Theoretical and experimental bearing torques vs. the preload magnitude; (b) Experimental bearing torques vs. contact loads; (c) Experimental bearing torques vs. the maximum Hertz stresses of the contact point. M_{sc}: calculated bearing torque; M_{bm}: measured bearing torque; M_{sm}: measured starting torque

occurs because of the curved shape of the contact area. Therefore, this S-shaped experimental curve indicates that the rolling resistance results from not only the elastic hysteresis losses in the metal, but also from the friction due to interfacial slip. Nevertheless, the friction and the resultant bearing torque that arises from gross sliding, that is, spinning of the ball on the race, is far greater than the loss due to hysteresis effects.

4. The results of experimental rolling frictional torque are in good agreement with the theoretical predictions. This demonstrates the feasibility of the present mathematical model.

Fig. 9b shows the relationship between the bearing torque and the contact loads. Fig. 9c provides an example of the maximum Hertz contact stress at the contact point No. 2. From Figs. 9a and 9b, the distributions of the curves are also S-shaped. These results demonstrate that the plastic deformation is always yielded by repeated loads and high local stresses (Willner, 2004; Williams, 2005).

In practice, to meet the requirement of this type of aircraft simulating rotary table, including high rigidity, high precision and high capability against overturning, the starting torque is often controlled in the range of 90–100 N·m. The corresponding preload magnitude is 130–140 μm (Fig. 9b). The preload magnitude obtained by our previous numerical method, however, is 10–158 μm (Shan *et al*., 2007b). As the range of 130–140 μm is narrower, this implies that the present method can more effectively prevent rolling noise, overturning moments and wear of the wire race ball bearing. This further demonstrates that the present method can more exactly control the preload of the wire race ball bearing.

4.2 Post test inspection

After the experiments, a conforming groove was observed around the circumference of the wire raceways. Fig. 10 illustrates a scanning electron microscope (SEM) picture of the contact indentation on the contact surface of a wire race. From Fig. 10, one can conclude that plastic deformation occurred in the contact zones of wire races. The plastic deformation can change the geometry of the contacting surfaces, and hence, the load transfer ratios and contact stresses.

In applied engineering, the contact stresses between the wire races and balls increase with increasing normal contact loads. The plastic deformation occurs with elastic deformation. In addition, the plastic deformation will cause residual stress in the contact zone. The resulting residual stress can prevent further plastic deformation (Johnson, 1985). Therefore, to some extent, the plastic indentation contributes to defense and preservation of the contact bodies.

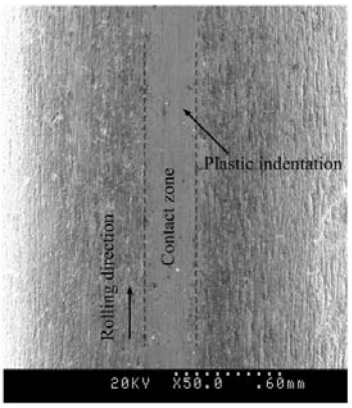

Fig. 10 SEM picture of the contact indentation on the contact surface of a wire race

5 Conclusions

1. In this paper, a more effective approach for exactly determining the preload of a wire race ball bearing was explored. A new mathematical model of the preload and the starting torque of the wire race ball bearing was developed, based on the 3D rolling friction resistance and the non-conforming contact theory.

2. The analytical results obtained by a numerical computation in MATLAB® and the experimental results showed that the preload magnitude can be controlled in the range of 130–140 μm by the present method. This is more precise than the preload range 10–158 μm achieved by a previous numerical method, and can more effectively prevent from rolling noise, overturning moments and wear of the wire race ball bearing.

3. This work provides significant theoretical and experimental supports for the engineering application of the wire race ball bearing with a large diameter in aircraft simulating rotary table.

References

Anderson, W.J., 1964. Rolling-element Bearings, Advanced Bearing Technology. Bisson, E.E., Anderson, W.J. (Eds.), NASA SP-38, p.139-173.

Drutowski, R.C., 1959. Energy losses of balls rolling on plates. *Journal of Basic Engineering, Series D*, **81**(2):233-238.

Drutowski, R.C., 1962. The Linear Dependence of Rolling Friction on Stressed Volume, Rolling Contact Phenomena. Bidwell, J.B. (Ed.), Elsevier Publishing Co., Amsterdam, p.113-131.

Drutowski, R.C., Mikus, E.B., 1960. The effect of ball bearing steel structure on rolling friction and contact plastic deformation. *Journal of Basic Engineering*, *Series D*, **82**(2):302-308.

Fan, S.L., 2005. The structure design of azimuth branch sustatined rotating device in some big antenna pedestal. *Modern Radar*, **27**:67-70 (in Chinese).

Gao, Y.F., Bower, A.F., Kim, K.S., Lev, L., Cheng, Y.T., 2006. The behavior of an elastic-perfectly plastic sinusoidal surface under contact loading. *Wear*, **261**(2):145-154. [doi:10.1016/j.wear.2005.09.016]

Jamari, J., Schipper, D.J., 2006. An elastic-plastic contact model of ellipsoid bodies. *Tribology Letters*, **21**(3):262-271. [doi:10.1007/s11249-006-9038-3]

Jamari, J., Schipper, D.J., 2007. Plastic deformation and contact area of an elastic-plastic contact of ellipsoid bodies after unloading. *Tribology International*, **40**(8):1311-1318. [doi:10.1016/j.triboint.2007.02.015]

Johnson, K.L., 1985. Contact Mechanics. Cambridge University Press, Cambridge.

Jones, A.B., 1952. The life of high-speed ball bearings. *Transactions of the ASME*, **74**(5):695-703.

Kogut, L., Etsion, I., 2002. Elastic-plastic contact analysis of a sphere and a rigid flat. *Journal of Applied Mechanics, Transactions of the ASME*, **69**(5):657-662. [doi:10.1115/1.1490373]

Lamon, P., Krebs, A., Lauria, M., Siegwart, R., Shooter, S., 2004. Wheel Torque Control for a Rough Terrain Rover. Proceedings of IEEE International Conference on Robotics and Automation, **5**:4682-4687. [doi:10.1109/ROBOT.2004.1302456]

Poritsky, H., Hewlett, C.W.Jr., Coleman, R.E.Jr., 1947. Sliding friction of ball bearings of the pivot type. *Journal of Applied Mechanics, Transactions of the ASME*, **14**(4):261-268.

Samper, V.D., Sangster, A.J., Reuben, R.L., Wallrabe, U., 1999. Torque evaluation of a LIGA fabricated electrostatic micromotor. *Journal of Microelectromechanical Systems*, **8**(1):115-123. [doi:10.1109/84.749410]

Shan, X.B., Tie, T., Chen, W.S., 2007a. Novel approach for determining the optimal axial preload of a simulating rotary table spindle system. *Journal of Zhejiang University-SCIENCE A*, **8**(5):812-817. [doi:10.1631/jzus.2007.A0812]

Shan, X.B., Xie, T., Chen, W.S., 2007b. A new method for determining the preload in a wire race ball bearing. *Tribology International*, **40**(5):869-875. [doi:10.1016/j.triboint.2006.09.003]

Shi, J., 2004. Design of the wire race ball bearing in a mini photoelectric search equipment. *Electronic and Electro-optical System*, **2**:33-35 (in Chinese).

Williams, J., 2005. The influence of repeated loading, residual stresses and shakedown on the behaviour of tribological contacts. *Tribology International*, **38**(9):786-797. [doi:10.1016/j.triboint.2005.02.006]

Willner, K., 2004. Elasto-plastic normal contact of three-dimensional fractal surfaces using halfspace theory. *Journal of Tribology, Transactions of the ASME*, **126**(1):28-33. [doi:10.1115/1.1631019]

Zhu, H.P., Yu, A.B., 2003. The effects of wall and rolling resistance on the couple stress of granular materials in vertical flow. *Physica A: Statistical Mechanics and Its Applications*, **325**(3-4):347-360. [doi:10.1016/S0378-4371(03)00143-2]

APPENDIX A

Due to the referee's suggestions, authors supply the detailed explanation for Eq. (1) and Fig. 2 here.

The contact model between the ball and the wire race can be treated as a quasi-static model associated with the rolling resistance. The contact bodies are mainly subjected to a normal contact load P, and a relative motion trend caused by a horizontal force F_v. Fig. A1 shows the sketch of the force diagram for a ball. In this case, contact deformation between the ball and the wire occurs. The contact point is expanded into a contact zone A, as illustrated by Fig. A2a. Fig. A2b shows the simplified force and the moment of rolling resistance couple.

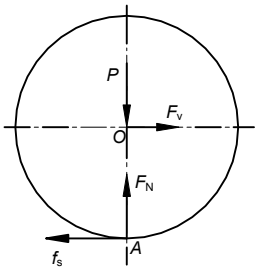

Fig. A1 Sketch of the force diagram for a ball

Thus, the rolling frictional resistance moment of couple M_r, the frictional force f_s, and the normal reaction force F_N in relationship to each other can be obtained, as shown in Fig. A2c. To better understand this point, Fig. A3 shows the ketch of the physical meaning for the coefficient of rolling frictional resistance. From Fig. A3, it can be found that the coefficient of rolling frictional resistance, ξ, relates the normal contact force to the rolling frictional resistance torque, and has units of length (Samper *et al*., 1999).

Therefore, according to the theorem of rolling frictional resistance, the relationship between the moment of rolling resistance couple, M_r, and the normal contact force, F_N, was expressed as

$$M_r=\xi F_N, \tag{1}$$

where ξ is the coefficient of rolling frictional resistance (m), which relates the normal contact force to the rolling frictional resistance torque, and has units of length (Samper *et al*., 1999).

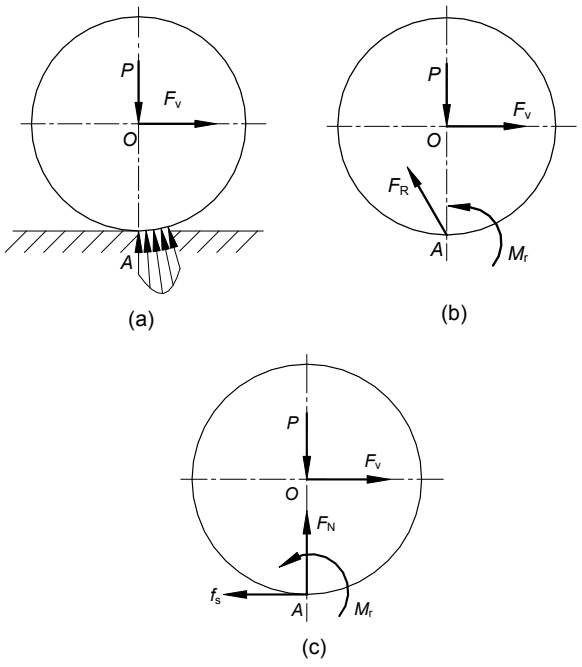

Fig. A2 Sketch of the rolling frictional resistance
(a) Contact deformation zone; (b) Simplified force and the moment of rolling resistance couple; (c) Decomposition of force

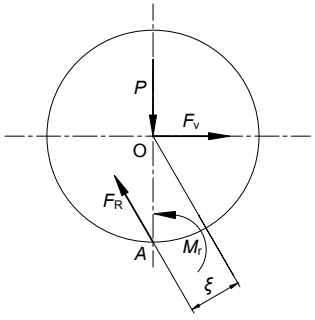

Fig. A3 Sketch of the physical meaning for the coefficient of rolling frictional resistance